

Benzaldehyde and 2-acetyl-1-naphthol were dissolved in 25 ml of ethanol, agitated at room temperature for an hour, and then 1.5 ml of a 40% KOH solution was added. The reaction mixture was then left at room temperature for the remainder of the day. The reaction mixture was then added to a bowl of ice-cold, diluted HCl-containing water. The resulting solid product was separated by filtering, recrystallized in ethanol, and then stored above CaCl₂.

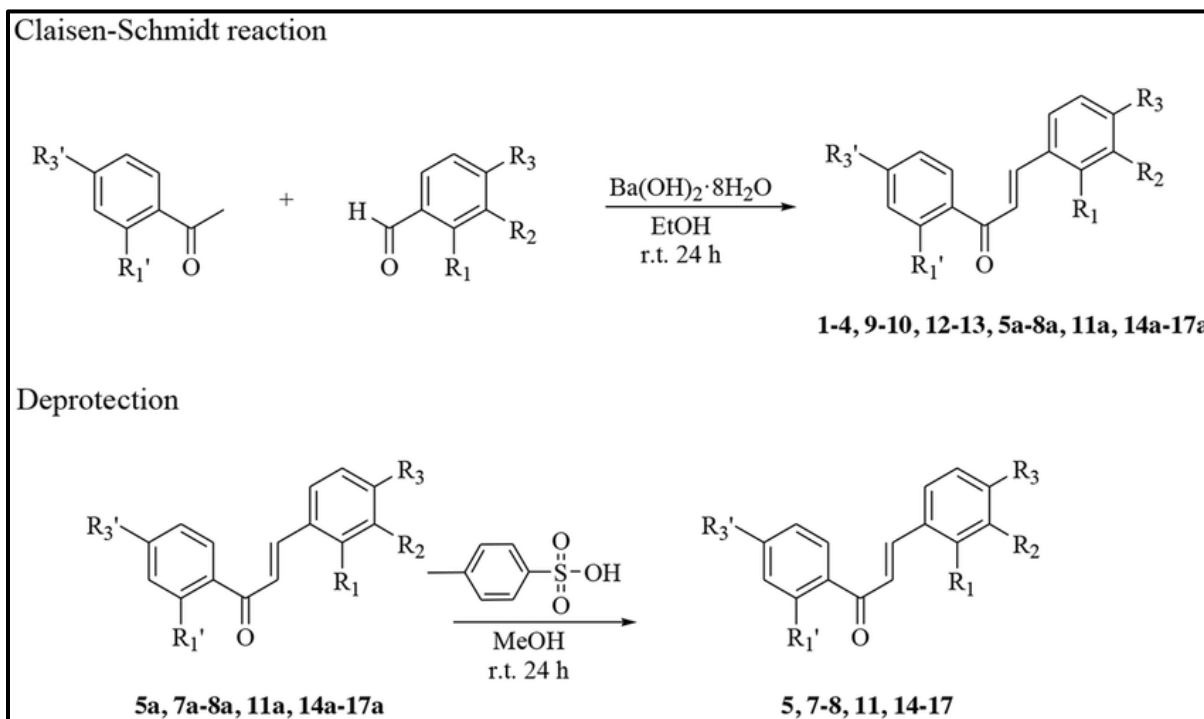


Figure. 1. Preparation of chalcone based ligand (Claisen- Schmidt condensation)

2.2 Preparation of tri-thiocarbonate ligand:

The carbon disulfide (CS₂) solution in DMF was mixed with an aqueous solution of potassium hydroxide (KOH) at a temperature of 15-20 °C to create the potassium salt of K₂CS₃.

2.3 Preparation of complexes

By using standard methods, the chalcone ligand was complexed with metal salts (Ferrous sulfate/Cobalt Chloride/Nickel Chloride). To make the metal chalcone complex, metal salt solutions in ethanol-water (1:1, V/V) were slowly applied to the ethanolic chalcone ligand solution with stirring. By slowly adding a saturated ethanolic-water solution of copper sulfate/Zinc acetate to a solution of a tri-thiocarbonate ligand, the salts were formed. The resulting products were filtered and vacuum-dried.

Physical measurement and analysis

Elemental analyses (C, H, and N) were carried out on a Carlo Erba 1108 component analyzer. The complex's organic component was broken down using conc. HNO₃, and the metal and sulphur were quantified using conventional gravimetric methods. Uncorrected measurements of the melting point were made in an open capillary. Purity and reaction progress were tested using TLC on silica gel

plates. FT-IR spectra were collected on an FT-IR Nicolet 510 spectrometer using the standard KBr disc technique over the range of 500- 4000 cm^{-1} with a resolution of 4 cm^{-1} , and ^1H & ^{13}C -NMR spectra were recorded 600 MHz models using DMSO- d_6 .

The complexes' powder XRD spectra were obtained at room temperature on a Seifert model ID-300 with a nickel channel ($\lambda = 1.5406$). The XRD designs were estimated to be 2 in the 20-90 scale. Using Bragg's condition $n = 2d\sin\theta$, where n is the order of reflection and θ is the angle of reflection, the interlayer dispersion d was identified. Using two test systems, the Keithley 236 source measure unit and the Schlumberger Impedance/Gain stage evaluation model (Si-1260), the electrical conductivity of packed pellets in the buildings was evaluated (SMU). The block was evaluated at a repetition rate of 1 kHz using a heap of 20 KN and a course of circular plate-shaped pellets secured with Elteck's silver paste for electrical contact. Inside, the temperature was kept at a controlled 1°C range.

RESULTS AND DISCUSSION

4.1 FT-IR SPECTRA

The Absorption band of aromatic (-OH) actually can be seen in IR spectra of ligand 3420 cm^{-1} . This show that just one of the phenolic oxygen from every one of the ligand is deprotonated and engaged with coordination with metal moreover, the band showed up in IR scale 1307 - 1270 cm^{-1} because of IR phenolic C-O stretching in free chalcone ligand has been downward shifted and spectra of the complexes demonstrating the coordination through phenolic oxygen in the bonding of metal are upheld by the presence of new band $\nu(\text{C-O-M})$ in range of 865-988 cm^{-1} . The complexes and ligand show IR bands stretching frequency in the range of 2933-3000 cm^{-1} , 2467-2512 cm^{-1} , and 1122-1618 cm^{-1} corresponding for ($=\text{CH}$ of Ar), ($-\text{CH}=\text{CH}$) and ($-\text{C}=\text{O}$) group of the chalcone based ligand and bands at 1287-1318 cm^{-1} , 865-988 cm^{-1} and 765-795 cm^{-1} for ($-\text{C}=\text{S}$), ($-\text{C-O-M}$) and ($-\text{C-S-M}$) bands of a tri-thiocarbonate ligand. The presence of coordinates water is also supported by FT-IR spectra of the complexes.

4.2 NMR spectra

The NMR spectra of the complexes were recorded in DMSO- d_6 , ^1H & ^{13}C -NMR data are recorded as Table 3. The presence of aromatic proton is confirmed by the multiple in between 7.06 - 8.46 ppm, $-\text{CH}=\text{CH}-$ band has been confirmed by the signal in a range of 7.10-8.38 ppm. While singlet peak of a hydroxyl group in the ligand (L) at 10.80 but due to complexation (-OH) peak not observed in complexes and ^{13}C -NMR signals appears at the range of 128.00- 164, 114.16 – 148 and 180.02 - 198.48 of (Ar-C), ($-\text{C}=\text{C}-$ of ethylene carbon) and α,β -unsaturated ketones ($-\text{C}=\text{O}$).

4.3 Electronic spectra

Due to the $n \rightarrow \pi^*$ transformation of α,β -unsaturated ketones, the UV-Visible spectra display absorbance in the range of 220-480 nm. Bathochromic shift causes a compound with a double bond moiety, i.e. a chromophoric group ($-\text{C}=\text{O}$), to absorb at a higher wavelength. The $n \rightarrow \pi^*$ transition in aromatic 256 nm causes the B-band to appear.4.4

4.4 Magnetic susceptibility

The table shows the magnetic moment values of the complexes. 5. Magnetic susceptibility of complexes evidence indicates that Cu(II) has a square planar geometry, while Ni(II), Co(II), and Fe have octahedral geometry (II).

4.5. Solid state electrical conductivity

The complexes' temperature-dependent solid-state electrical conductivity demonstrates their semiconducting existence. The conductivity of water increases as the temperature rises. This behaviour may be explained by the existence of exocyclic sulphur in CS32-, which forms short M—S and S—S interactions.

4.6 Powder XRD Spectra

Figures 2-3 demonstrate the powder X-ray diffraction patterns of the complexes. Small variations in 2θ and d-spacing, lattice strain, crystallite size, and peak intensity have been observed in the patterns. The crystallinity of the complexes is determined by contrasting background patterns to sharp peaks in the powder XRD diffraction of the sample. The complexes' crystalline existence is shown by their powder XRD patterns (Figures 2 and 3).

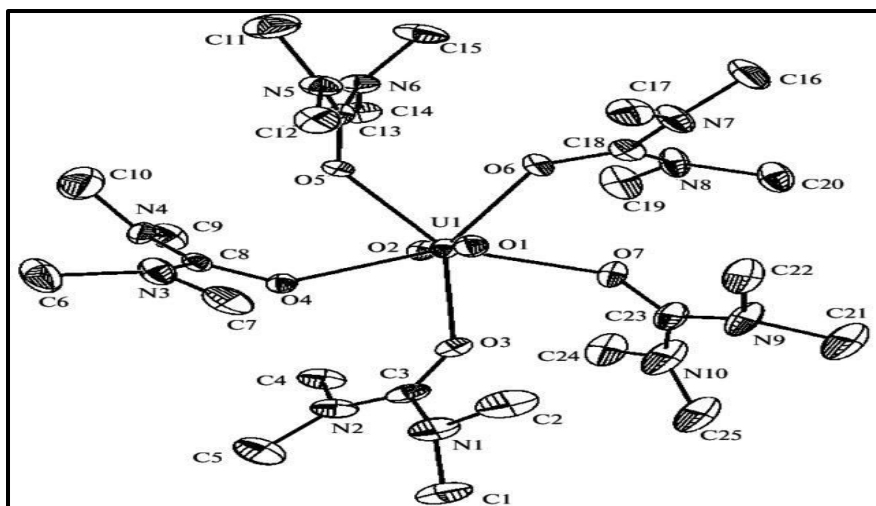


Fig. 2 [Cu(CS3)2][Ni(L)2(H2O)2]

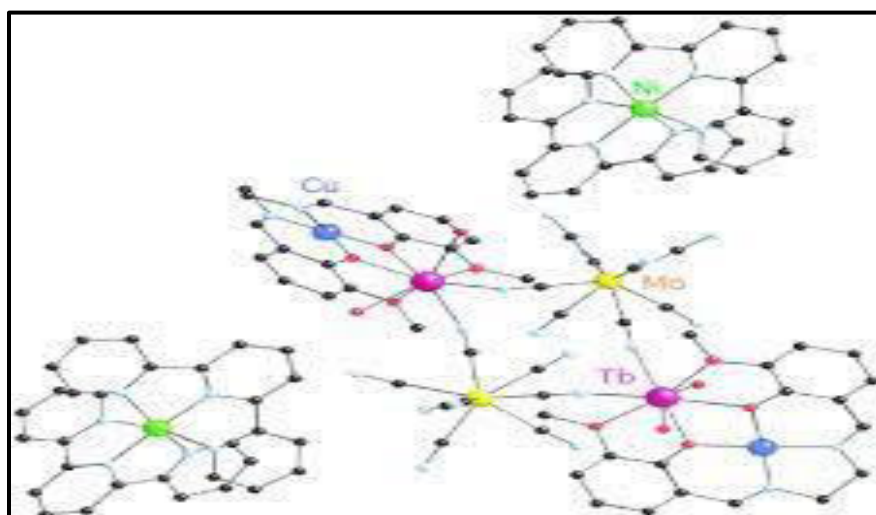


Fig. 3 [Zn(CS3)2][Ni(L)2(H2O)2]

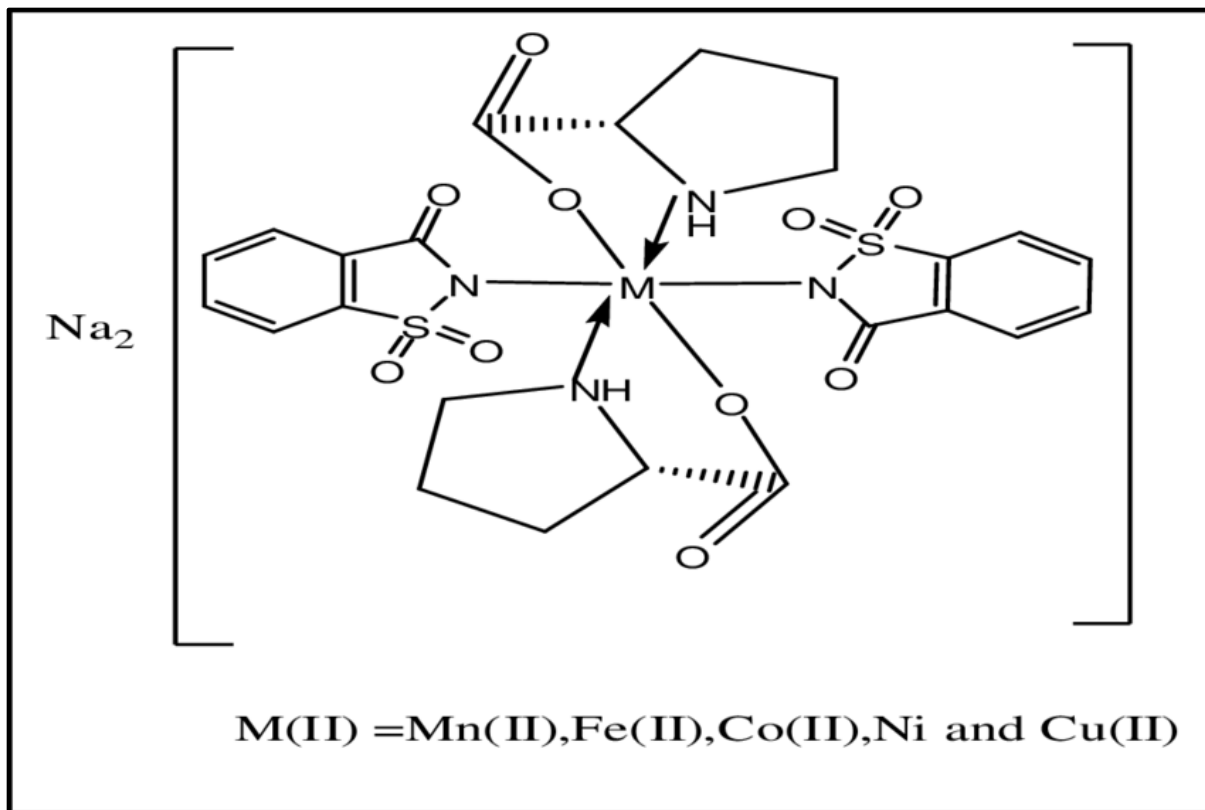


Figure. 4 Proposed structure of the complexes

Conclusion:

Electronic absorption specifications and magnetic susceptibility measurements are met by the anionic metallo ligand $[\text{M}(\text{CS}_3)_2]^-$. The square planar shape of the core metal atom $[\text{M} = \text{Cu(II)}$ or Zn(II)] is evident. In the cationic component of the complex salt, the central metal atom $[\text{Fe(II)}/\text{Ni(II)}$ or $\text{Co(II)}]$ is assumed to be in octahedral geometry. An IR peak confirms the presence of organised water. According to studies on temperature-dependent solid-state conductivity, these substances are semiconductors. Stepwise temperature increases have been seen to increase conductivity. There is probably contact between $\text{M}-\text{S}$ and $\text{S}-\text{S}$.

REFERENCE:

1. Kou, ShanShan, et al. "Synthesis, characterization and theoretical investigation of the structure, electronic properties and third-order optical nonlinearity of $\text{M}(\text{dnpi})_2$ ($\text{M} = \text{Cu}^{2+}$, Co^{2+} and Pb^{2+} ; $\text{dnpi} = 4, 5$ -Diphenyl-2-(4-nitrophenyl)-1H-imidazole)." *Dyes and Pigments* 104 (2014): 102-109.
2. Mahapatra, Debarshi Kar, et al. "Perspectives of medicinally privileged chalcone based metal coordination compounds for biomedical applications." *European journal of medicinal chemistry* 174 (2019): 142-158.
3. Cinteza, Ludmila-Otilia, and Maria Marinescu. "Synthesis and nonlinear studies on selected organic compounds in nanostructured thin films." *Advanced Surface Engineering Research. London: IntechOpen* (2018): 1-23.

4. Majumdar, Dhrubajyoti, et al. "A rare hetero-bimetallic Zn (II)/Ca (II) Schiff base complex: Synthesis, crystal structure, DFT, molecular docking and unveiling antimicrobial activity." *Journal of Molecular Structure* 1222 (2020): 128951.
5. Plants, Selected Medicinal. "Doctoral Theses."
6. Budnikova, Yulia H., et al. "Considerations on electrochemical behavior of NLO chromophores: Relation of redox properties and NLO activity." *Electrochimica Acta* 368 (2021): 137578.
7. Baghaffar, Gameel A., et al. "Synthesis, characterisation and thermal stability of 2-ferrocenylidene (1-tetralone), 2-ferrocenylideneindan-1, 3-dione, diferrocenylidene cyclohexanone and diferrocenylidene cyclopentanone." *Pigment & Resin Technology* (2008).
8. Sarmah, Bhaskar, and Rajendra Srivastava. "Octahedral MnO₂ Molecular Sieve-Decorated Meso-ZSM-5 Catalyst for Eco-Friendly Synthesis of Pyrazoles and Carbamates." *Industrial & Engineering Chemistry Research* 56.51 (2017): 15017-15029.
9. Ghosh, Avishek, et al. "Electrolyte-Free Dye-Sensitized Solar Cell with High Open Circuit Voltage Using a Bifunctional Ferrocene-Based Cyanovinyl Molecule as Dye and Redox Couple." *Organometallics* 37.13 (2018): 1999-2002.
10. Tegoni, M., et al. "Copper chelators: chemical properties and bio-medical applications." *Current medicinal chemistry* 21.33 (2014): 3785-3818.
11. Gritzner, G., and J. Kuta. "Recommendations on reporting electrode potentials in nonaqueous solvents (Recommendations 1983)." *Pure Appl. Chem* 56.4 (1984): 461-466.
12. de Krom, Iris Maria Johanna. "Synthesis, characterization, and reactivity of novel transition metal complexes based on aromatic phosphorus heterocycles."
13. Salas, Paloma F., Christoph Herrmann, and Chris Orvig. "Metalloantimalarials." *Chemical reviews* 113.5 (2013): 3450-3492.
14. Singh, Meenakshi. *Design, synthesis and biological evaluation of some novel benzothiazole derivatives*. Diss. 2016.
15. Munir, Rubina, et al. "Microwave-Assisted Synthesis of (Piperidin-1-yl) quinolin-3-yl) methylene) hydrazinecarbothioamides as Potent Inhibitors of Cholinesterases: A Biochemical and In Silico Approach." *Molecules* 26.3 (2021): 656.